Journal of Applied Research on Industrial Engineering

Paper Type: Research Paper

Investigation of Charge Carrier Transport and Recombination in Organic Semiconductors with Charge Extraction by Linearly Increasing Voltage (CELIV) Technique

Ali Mahmoudloo* [iD]

Department of Basic Science, Farhangian University, Tehran, Iran; mahmodlou_ali@yahoo.com.

Abstract

This study aimed to calculate the drift velocity and mobility of holes in organic semiconducting polymers by the Charge Extraction via Linearly Increasing Voltage (CELIV) technique to measure the charge carrier mobility. The charge carrier mobility is defined as carrier drift velocity v in each electric field E. This technique is complementary to Time of Flight (ToF) by providing us with an indication of the material's properties when other methods are not applicable. Typically, Photo-CELIV is used to measure the charge carrier mobility in Organic Semiconductor (OSCs) due to large bandgap (2 eV) and few thermally generated carriers for extraction in the dark. The effect of the recombination mechanism is investigated on the carrier mobility in the organic layer. The calculation results showed that saturation of extracted charge is linearly proportional to carrier concentration at low concentrations, whereas at high density is saturated due to bimolecular carrier recombination. Langevin recombination mechanisms show that extracted demand saturates at j_0, the capacitive displacement current step. Therefore, $\Delta j/j_0 = 1$ at high light intensities, the saturation of extracted charge will start to decrease from its maximum value only when t_{del} is increased to be like t_{max}. In Langevin recombination, the bimolecular carrier lifetime is much faster than transit time at high carrier concentrations giving the saturation of extracted charge.

Keywords: CELIV technique, Organic semiconducting, Charge carrier transport, Time of flight.

1 | Introduction

Organic Semiconductor (OSCs) share standard features. All crystals have van-der-Waals bonded, whereas the intermolecular interactions are much weaker than the intramolecular bonds. Individual molecules are well separated with van-der-Waals distances of 3.8 to 4Å. These materials' structural and mechanical behaviors are remarkably different from inorganic materials due to weak bonding. For instance, hardness is usually lower than inorganic materials, and the thermal expansion coefficients are more significant [1].

OSCs mainly come in two varieties of small molecules and polymers. As the name suggests, small molecules are relatively small molecular weight molecules with conjugated carbon atoms, which can be prepared as single molecular crystals. The molecules in these crystals are tightly coupled in their π-

systems, resulting in unique transport properties with mobilities of 1-10 $\frac{cm^2}{VS}$. Most molecules can be quickly evaporated to form polycrystalline layers. Organic semiconducting polymers are long chains of conjugated carbon atoms composed of smaller repeating units called monomers. Modified polymers can be self-organized when deposited from solution at room temperature, resulting in a relatively high mobility layer that can be used to print circuits at low cost [2], [3].

Measurement of the fundamental limits of charge carrier mobilities in OSCs is crucial for developing organic electronics. However, devices such as Organic Field Effect Transistors (OFETs), Organic Thin Film Transistors (OTFTs), and Organic Light-Emitting Diodes (OLEDs) are already used in commercial applications. There still needs to be a complete understanding of these devices' final limitations of performance and stability. Growing ultra-pure, fully ordered molecular crystals requires determining the electronic properties of OSCs. The organic crystals show mobilities as high as amorphous silicon. Dislocations and grain boundaries, which may limit charge transfer, are essential in these crystals [4]. Thermal expansion should be considered when devising crystal growth procedures since the (often anisotropic) expansion tensor produces large stress/strain fields in the presence of temperature gradients. Charge carrier transport in OSCs has been investigated for over three decades. The most crucial charge transport features directly follow from the basic structural features of organic glasses. While these glasses are molecular materials, their position and orientation are disordered because of weak interactions between molecules. All relevant states are localized, and charge carrier transport occurs by the hopping mechanism. Hopping transport is an essential method for disordered materials [5].

The recent success of OLEDs in display technology further increases the demand for "all-organic" electronics. Organic electronic circuits driving organic displays would greatly benefit the manufacturing process if they were made of organic materials. The past decade has seen substantial progress in this field. Organic molecules with extended π-conjugation have been successfully used as active semiconductors in devices like OFETs.

However, an adequate understanding of the physical principles governing charge transport in organic materials still needs to be included. In disordered polymeric organic materials, the hopping transport of electrons and holes prevails. Karl et al.'s classical experiments demonstrated a "band-like" transport mechanism for both charge carriers in highly ordered, ultra-pure organic single crystals of mm-sized dimensions. However, the concept of band-transport successfully used to describe charge transport in conventional in OSCs like Si and GaAs is inappropriate for OSC materials. Previous theoretical research has demonstrated that the electronic bands in OSCs are essentially flat. For such a situation, the conventional description predicts impaired charge carrier mobility – the figure of merit of semiconductor materials. Recent advances in the theoretical description of charge transport in organic materials have shown that a completely different physical picture is needed to describe charge transport in organic materials.

Most importantly, lattice vibrations should be considered explicitly. Hamiltonians have been established for the ordered crystalline systems models, where the interaction between molecules and the lattice dynamic is parametrized. In more disordered systems, parametrization is more complex, and these methods are less predictive. A precise description of charge transport phenomena requires an atomistic simulation for the actual structure (i.e., including thermal vibrations). There are two main approaches to this problem. It is possible to extract charge transfer parameters from a molecular dynamics' morphology simulation. These are then further used in hopping models to describe the movement of the localized charge from one molecule to the other. The second path propagates the electronic degrees of freedom using the time-dependent Schrödinger equation, whereas the cores are propagated classically with non-adiabatic simulation schemes [6].

A deeper understanding of OLED, organic solar cells, and nanoscale molecular electronics requires knowledge of charge transport in organic materials. Developing organic molecules with high mobilities and guiding principles to construct organic molecules with high mobilities is urgently needed. In addition, the need for rules with predictive power, allowing for a rational design and synthesis of molecules with high charge carrier mobilities, is pressing. A simplistic guiding principle is "best mobility values are obtained for planar molecules where π–π-interactions allow an optimal stacking". This principle is valuable but sometimes tricky to apply when explaining that some molecules show the highest mobilities and deviate substantially from planar geometries (e.g., rubrene). Therefore, searching for organic molecules with high charge carrier mobilities has remained a trial-and-error effort [7].

This paper briefly overviews organic photovoltaic devices and charge transfers through the active layers. Then the photo-induced charge carrier extraction is introduced by linearly increasing voltage (photo-Charge Extraction via Linearly Increasing Voltage (CELIV)) technique to give comprehensive indications of charge carrier mobility, density, and recombination in organic photovoltaics. The photo-CELIV characterization is shown using extraction current transients to understand degradation mechanisms through observation of the trapping of charge carriers and bimolecular recombination. In addition, some examples of deployment and interpretation of the results are given. It is hoped that this brief introduction serves as a stepping stone into more in-depth papers and books and encourages more extensive use of photo-CELIV technology, which can be employed with whole devices.

2 | Calculation and Model

CELIV is a powerful method allowing charge transport and recombination to be studied in various semiconductors. This complimentary technique allows studying materials when other techniques, such as Time of Flight (ToF), are inapplicable [8].

The advantages are: 1) strongly dispersive transport in disordered semiconductors can be probed, whereas featureless exponential decay is observed in ToF, 2) extraction time t_{max} is still visible in strongly dispersive transport (in ToF, the position of the kink is not clear even in the log-log scale), 3) films with high intrinsic conductivity can be studied, whereas, in ToF, only films with low conductivity can be measured, and 4) recombination processes can be studied [9], [10].

The equation to calculate charge carrier mobility with surface photo-generated small charge was derived:

$$t_{tr} = d\sqrt{2/\mu A} \, . \tag{1}$$

Organic electronic devices, such as solar cells and light-emitting diodes, are typically very thin, hundreds of nanometers. Therefore, charge carriers are photo-generated in the volume of the films based on the Beer-Lambert law. In addition, charge carrier distribution due to doping is typically homogeneous throughout the film [11].

$$t_{max} = \frac{t_{tr}}{\sqrt{3}} = d\sqrt{2/3\mu A} \, . \tag{2}$$

The case of high conductivity, carrier extraction:

$$t_{max} = \sqrt[3]{t_{tr}^2 \tau_\sigma / 2} = \sqrt[3]{\tau_\sigma d^2 / \mu A} \, . \tag{3}$$

A correction factor to estimate the carrier mobility for intermediate film conductivities again in case of carrier extraction from the film was published later as determined from numerical calculations [12].

$$t_{max} = d \sqrt{\frac{2}{3\mu A(1 + 0.36\frac{\Delta j}{j_0})}} , \qquad (4)$$

where μ is the mobility of the OSC, d is layer thickness, A is layer area, t_{tr} is transit time, and σ is conductivity.

Further, Deibel and Bange showed that the correction factor should be slightly different, which would change the results much less than the experimental error. CELIV transients and the extraction time depend on carrier bimolecular recombination and carrier concentration, which should be considered and accounted for in mobility calculations [13], [14]. This work was further extended to account for all possible experimental parameters, namely light absorption profile, charge carrier concentration, and bimolecular recombination. Calculating the charge carrier mobility in the CELIV experiment is discussed below, accounting for all these experimental conditions.

A typical CELIV setup is like ToF, except when ToF can be (though usually is not) measured with large load resistances (integral mode ToF). CELIV can only be done in differential mode when the load resistance is low (RC < ttr) [15].
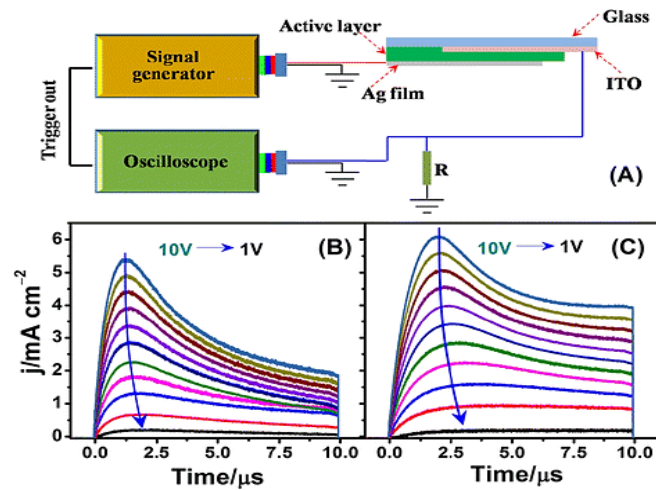

Fig. 1. Schematic experimental setup and typical CELIV transients.

A triangle-shaped increasing voltage pulse is applied, and the current response is measured as a voltage change in the load resistance of the oscilloscope.
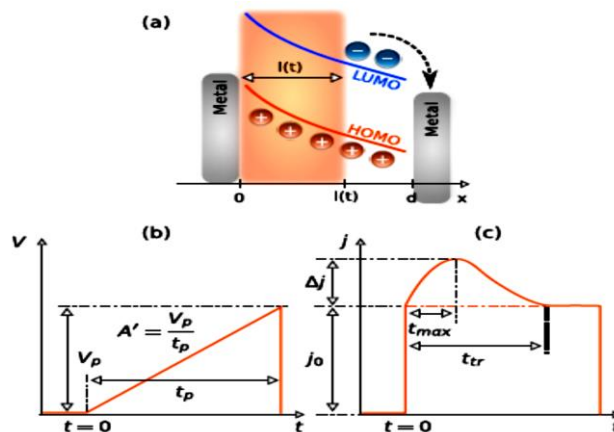

Fig. 2. Schematic illustration of the CELIV method: a) process of the charge extraction; b) scheme of the voltage input; c) the current output.

Two types of CELIV experiments can be done: [16].

   I.   Extraction of equilibrium generated (because of doping) carriers.

  II.   Extraction of photo-generated carriers, photo-CELIV, which is used for undoped films, when no thermally generated (equilibrium) carriers exist.

Typically, Photo-CELIV is used to measure the charge carrier mobility in OSCs since they are large band gaps (2 eV or so) and few thermally generated carriers are present for extraction in the dark [17], [18].

The essence of this technique to measure the charge carrier mobility is very simple. The charge carrier mobility is defined as carrier drift velocity v in each electric field E:

$$v = \mu.E. \tag{5}$$

From classical mechanics, the constant speed of a moving object is defined as the time required to travel the distance d:

$$v = d / t. \tag{6}$$

In our case, the distance is the film thickness, and time is the transit time:

$$\mu = \frac{v}{t_{tr}E} = \frac{d^2}{t_{tr}U}. \tag{7}$$

The transit time is required to extract the small number of charge carriers (less than CU) from the surface through the film. While an applied electric field pulls carriers, the current is observed in the external circuit and recorded in the oscilloscope. When all pages reach the opposite electrode, the extraction current drops to zero, and the extraction time is recorded from which carrier mobility is calculated. However, in CELIV, the electric field is non-constant, carrier generation might not be at the surface, and the time at the maximum extraction current is taken for mobility calculations, which require complex analysis. Similarly, as in ToF, the mobility of both electrons and holes can be measured from CELIV. Due to Beer-Lambert law, an essential requirement is to fulfill the surface carrier generation, which can be conducted by making film thickness much larger than the photogeneration profile (d >> αd). As shown in *Fig. 3*, the extraction of electrons or holes through the film can be selected by applying forward or reverse bias, or, if forward bias injects shows too heavy injection, the illumination from different electrodes can be done keeping the same applied bias [19]–[21].
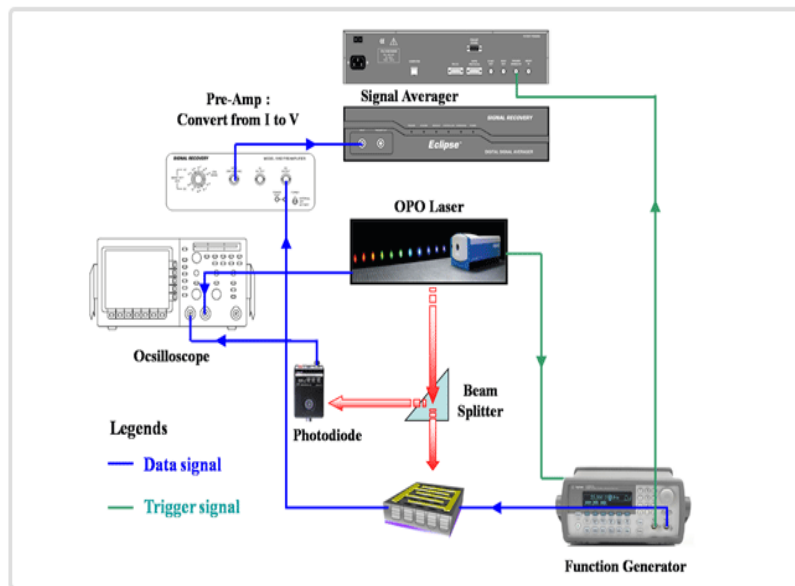

Fig. 3. Schematic measuring the mobility of electrons and holes.

3 | Results and Discussion

The disadvantage of this experiment is that typically thick films, like micrometers or more, are required. The typical thickness of organic electronic devices is much less, meaning that typically the faster carrier mobility can only be measured from CELIV in operational devices [22], [23].

The numerical calculations were used to simulate the experimental conditions and derive the correction factor to account for by the universal equation to calculate the mobility of photo-generated charge carriers in all possible empirical cases:

– *Light absorption profile.*
– *Carrier concentration.*
– *Langevin-type bimolecular recombination.*

While no analytical solution for the correction factor presently exists, the following graph can be conveniently used to correctly calculate the charge carrier mobility in systems with Langevin bimolecular charge carrier recombination (typically, most materials with carrier mobility < 1 cm2/V/s).
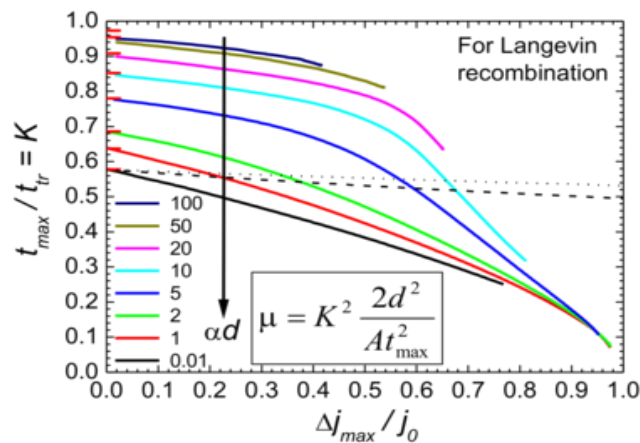

Fig. 4. Calculating charge carrier mobility with Langevin bimolecular charge carrier recombination.

The Δj will saturate to the capacitive displacement current step j_0, therefore $\Delta j / j_0 = 1$ at high light intensities (*Fig. 4*).

The easiest way to calculate the charge carrier mobility is in boundary cases: either in very thin or thick films at low carrier concentration (minor charge mode). *Fig. 4* shows that the correction factor becomes either K=2 for surface photogeneration and 2/3 for volume generation, precisely as derived in the past.

By inserting the field dependence of mobility, we get the field-dependent transport equation [24], [25]:

$$\frac{\partial}{\partial x}\left(\mu_0\left(\frac{\beta\left(\frac{\partial V}{\partial x}\right)^{\frac{1}{2}}}{KT}\right)V\frac{\partial V}{\partial x}\right) = \frac{\partial V}{\partial t}.. \tag{8}$$

In this formulation, the room temperature transient time is considered, the result of which is shown in *Fig. 5.*
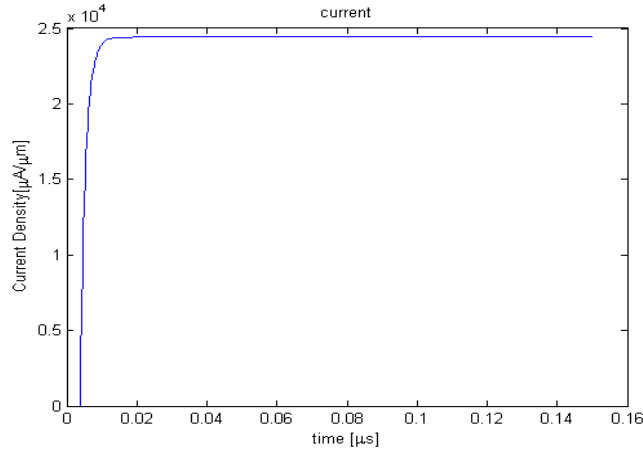
Fig. 5. Current density in simulating the transport of carriers along the organic layer.

We have used a simple model with a single trap level characterized by a carrier lifetime [25], [26].

$$\frac{1}{e}\frac{\partial J_p}{\partial X} + \frac{\partial p}{\partial t} = \frac{p - p_0}{\tau}. \tag{9}$$

One of the most significant advantages of CELIV is the ability to measure the concentration of photo-generated charge carriers at various delay times or light intensities. The presence of bimolecular carrier recombination and at what light intensity it starts to dominate can be estimated from *Fig. 6* shown below when ⊿j deviates from linear dependence. Unfortunately, only a very rough estimate of concentration can be made.

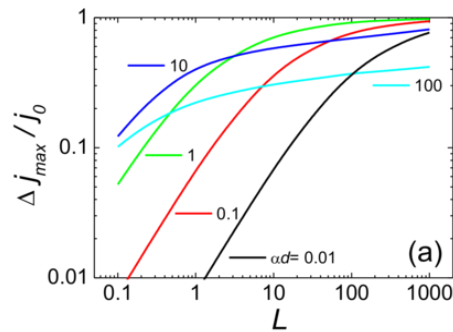Fig. 6. Carrier lifetime and recombination measurement, the Δj will saturate to the capacitive displacement current step j₀; therefore, Δj/j₀=1 at high light intensities.

Fig. 6 represents the transient response in a single trap, while the carriers' lifetime is about 5-10 nanoseconds. Lifetimes should be larger than or equal to the delay time because the holes are transported across the layer before they get trapped. The steady-state current decreases as the lifetime are reduced because of reducing the number of carriers contributing to conduction by trapping.
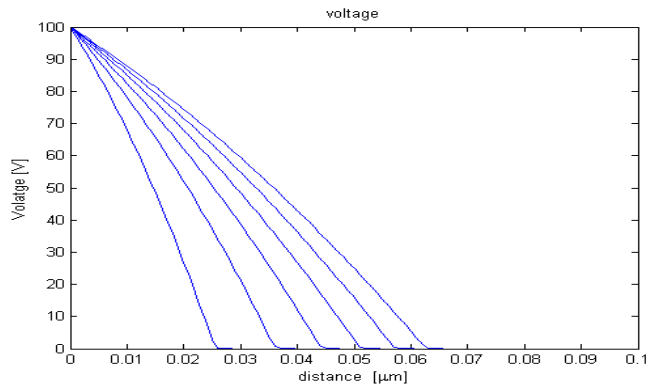

Fig. 7. Voltage behavior simulation of transport of carriers along the organic layer in intervals of 10 nanoseconds.

The pulse voltage response is shown in *Fig. 7* along the organic layer with ToF configuration by increasing the thickness of the layers so that the pulse voltage decays and shows a linear profile before it reaches the collector electrode.

Significant progress has been achieved in developing novel materials and new device engineering in the last decade. Arylene diimide families have shown high promise as helpful building blocks for fabricating next-generation electronic and optoelectronic devices to understand their transistor characteristics at the molecular scale to practical applications from medicine to high-end security systems. These organic compounds are being developed for improved resistance to thermal and environmental stresses, which is one of the significant challenges in the field. Several other combinations based on fullerene (C60) and chemically modified thiophenes are also being explored and developed for use in many devices encompassing interdisciplinary research areas. These devices are expected to pave the way for next-generation electronics with energy-efficient security systems, sensors, photonics, and spintronic memories due to their low cost and ease of synthesis and processing. This chapter briefly reviewed the different types of organic devices, their fabrication processes, and their recent applications by citing examples of oligomers and polymers.

4 | Conclusions

The calculation results show that saturation of extracted charge (Δj) is linearly proportional to carrier concentration at low concentrations, whereas, at high concentrations, it saturates due to bimolecular carrier recombination. When Langevin recombination mechanisms are present, the Δj will saturate to the capacitive displacement current step j_0; therefore, $\Delta j/j_0=1$ at high light intensities. Experimentally this saturation can be observed by changing the delay time t_{del} or laser intensity both control the carrier concentration when the extraction pulse is applied. The saturation of extracted charge decreases from its maximum value only when t_{del} is increased like t_{max} because the bimolecular carrier lifetime is much faster than transit time at high carrier concentrations giving the saturation of extracted charge in Langevin recombination. When $t_{del} = t_{tr}$, the extracted order will be approx= CU. The results demonstrated that only a time scale $> t_{tr}$ could be probed using CELIV when measuring carrier concentration decay with time. It is not the limitation of the CELIV technique, it is the nature of drift-governed carrier extraction from the films. Similar results would be observed in whatever electrical extraction method (for instance, using charge extraction with square-pulsed voltage).

References

[1] Kreouzis, T., Poplavskyy, D., Tuladhar, S. M., Campoy-Quiles, M., Nelson, J., Campbell, A. J., & Bradley, D. D. C. (2006). Temperature and field dependence of hole mobility in poly (9, 9-dioctylfluorene). *Physical review b*, *73*(23), 235201. https://doi.org/10.1103/PhysRevB.73.235201

[2] Majewski, L. A., Schroeder, R., Voigt, M., & Grell, M. (2004). Low voltage organic transistors on a polymer. *Journal of physics D: applied physics, 37*(3367), 337–347.

[3] Majewski, L. A., Schroeder, R., Grell, M., Glarvey, P. A., & Turner, M. L. (2004). High capacitance organic field-effect transistors with modified gate insulator surface. *Journal of applied physics*, *96*(10), 5781–5787.

[4] Steudel, S., De Vusser, S., De Jonge, S., Janssen, D., Verlaak, S., Genoe, J., & Heremans, P. (2004). Influence of the dielectric roughness on the performance of pentacene transistors. *Applied physics letters*, *85*(19), 4400–4402.

[5] Mahmoudloo, A., & Ahmadi-Kandjani, S. (2016). Variable range hopping transport characteristics of the charge carriers in homogenous amorphous organic semiconductors. *Optik*, *127*(3), 1265–1267. https://doi.org/10.1016/j.ijleo.2015.10.112

[6] Pankratov, E. L. (2022). Influence of missmatch-induced stress and porosity of materials on technological process. *International journal of research in industrial engineering (2783-1337), 11*(2), 92-118.

[7] Schrader, M., Körner, C., Elschner, C., & Andrienko, D. (2012). Charge transport in amorphous and smectic mesophases of dicyanovinyl-substituted oligothiophenes. *Journal of materials chemistry*, *22*(41), 22258–22264.

[8] Liu, C., Huang, K., Park, W. T., Li, M., Yang, T., Liu, X., … & Noh, Y. Y. (2017). A unified understanding of charge transport in organic semiconductors: the importance of attenuated delocalization for the carriers. *Materials horizons*, *4*(4), 608–618.

[9] Ucal Sari, I., & Ak, U. (2022). Machine efficiency measurement in industry 4.0 using fuzzy data envelopment analysis. *Journal of fuzzy extension and applications*, *3*(2), 177–191.

[10] Street, R. A., Northrup, J. E., & Salleo, A. (2005). Transport in polycrystalline polymer thin-film transistors. *Physical review B*, *71*(16), 165202. https://doi.org/10.1103/PhysRevB.71.165202

[11] Fritz, S. E., Kelley, T. W., & Frisbie, C. D. (2005). Effect of dielectric roughness on performance of pentacene TFTs and restoration of performance with a polymeric smoothing layer. *The journal of physical chemistry b*, *109*(21), 10574–10577.

[12] Shin, K., Yang, C., Yang, S. Y., Jeon, H., & Park, C. E. (2006). Effects of polymer gate dielectrics roughness on pentacene field-effect transistors. *Applied physics letters*, *88*(7). https://doi.org/10.1063/1.2176858

[13] Sosorev, A. Y. (2020). Simple charge transport model for efficient search of high-mobility organic semiconductor crystals. *Materials & design*, *192*, 108730. https://doi.org/10.1016/j.matdes.2020.108730

[14] Tunc, A. V., De Sio, A., Riedel, D., Deschler, F., Da Como, E., Parisi, J., & Von Hauff, E. (2012). Molecular doping of low-bandgap-polymer: fullerene solar cells: Effects on transport and solar cells. *Organic electronics*, *13*(2), 290–296.

[15] Panda, A., & Muniz, S. M. (2022). Smart home with neural network based object detection. *Big data and computing visions*, *2*(1), 40–48.

[16] Maennig, B., Pfeiffer, M., Nollau, A., Zhou, X., Leo, K., & Simon, P. (2001). Controlled p-type doping of polycrystalline and amorphous organic layers: Self-consistent description of conductivity and field-effect mobility by a microscopic percolation model. *Physical review B*, *64*(19), 195208. https://doi.org/10.1103/PhysRevB.64.195208

[17] Österbacka, R., Pivrikas, A., Juška, G., Poškus, A., Aarnio, H., Sliaužys, G., … Sariciftci, N. S. (2010). Effect of 2-d delocalization on charge transport and recombination in bulk-heterojunction solar cells. *IEEE journal of selected topics in quantum electronics*, *16*(6), 1738–1745.

[18] Gregg, B. A. (2009). Charged defects in soft semiconductors and their influence on organic photovoltaics. *Soft matter*, *5*(16), 2985–2989.

[19] Gregg, B. A. (2009). Transport in charged defect-rich π-Conjugated polymers. *The journal of physical chemistry c*, *113*(15), 5899–5901.

[20] Hamidzadeh, S. M., Rezaei, M., & Ranjbar-Bourani, M. (2022). A new dynamical behaviour modeling for a four-level supply chain: control and synchronization of hyperchaotic. *Journal of applied research on industrial engineering*, *9*(2), 288–301.

[21] Stelzl, F. F., & Würfel, U. (2012). Modeling the influence of doping on the performance of bulk heterojunction organic solar cells: One-dimensional effective semiconductor versus two-dimensional donor/acceptor model. *Physical review B*, *86*(7), 75315. https://doi.org/10.1103/PhysRevB.86.075315

[22] Kotlarski, J. D., Blom, P. W. M., Koster, L., Lenes, M., & Slooff, L. H. (2008). Combined optical and electrical modeling of polymer: fullerene bulk heterojunction solar cells. *Journal of applied physics*, *103*(8). https://doi.org/10.1063/1.2905243

[23] Liang, C., Wang, Y., Li, D., Ji, X., Zhang, F., & He, Z. (2014). Modeling and simulation of bulk heterojunction polymer solar cells. *Solar energy materials and solar cells*, *127*, 67–86.

[24] Rezzonico, D., Perucco, B., Knapp, E., Häusermann, R., Reinke, N. A., Müller, F., & Ruhstaller, B. (2011). Numerical analysis of exciton dynamics in organic light-emitting devices and solar cells. *Journal of photonics for energy*, *1*(1), 11005. https://doi.org/10.1117/1.3528045

[25] Ray, B., & Alam, M. A. (2012). Random vs regularized OPV: Limits of performance gain of organic bulk heterojunction solar cells by morphology engineering. *Solar energy materials and solar cells*, *99*, 204–212.